

DESCRIBING THE VALENCE-CHANGE TRANSITION BY THE DMFT SOLUTION OF THE FALICOV-KIMBALL MODEL

V. ZLATIĆ (zlatic@ifs.hr)

Institute of Physics, Bijenička c. 46, 10 001 Zagreb, Croatia

J. K. FREERICKS (freericks@physics.georgetown.edu)

*Department of Physics, Georgetown University, Washington,
DC 20057, U.S.A.*

Abstract. The anomalous properties of the YbInCu₄ family of intermetallic compounds are discussed and the experimental data are compared with the dynamical mean field theory (DMFT) of Falicov-Kimball model. We show that the DMFT provides a qualitative description of the valence-change transition and high-temperature behavior of these systems.

1. Introduction to Valence-Change Materials

Yb-based intermetallic compounds have an interesting isostructural valence-change transition (1, 2, 3, 4, 5, 6). Here, we briefly describe the most characteristic features of these systems, taking Yb_{1-x}Y_xInCu₄ as an example, and show that the Falicov-Kimball model provides a qualitative description of the experimental data.

At zero doping and ambient pressure the properties of YbInCu₄ are dominated by a first-order valence-change transition at about 40 K. The valence of the Yb ions changes from Yb³⁺ above T_v to Yb^{2.85+} below T_v (1, 7), where T_v is the transition temperature. and the lattice expands by about 5 %. The crystal structure remains in the C15(b) class and the volume expansion estimated from the atomic radii of the Yb³⁺ and Yb²⁺ ions is compatible with the valence change estimated from L_{III} -edge data (1, 8). Specific heat data shows a first-order transition at T_v with an entropy change $\Delta S \simeq R \ln 8$ corresponding to a complete loss of magnetic degeneracy in the ground state (4). Neutron scattering does not provide any evidence for long range order below T_v (9). Y-doping reduces T_v until a critical concentration of 15 % of Y ions is reached, where the high-temperature phase extends down to T=0 K (5, 6, 10). The experimental results for the

resistivity, susceptibility and thermopower (6) of $\text{Yb}_{1-x}\text{Y}_x\text{InCu}_4$ are shown in Fig. 1.

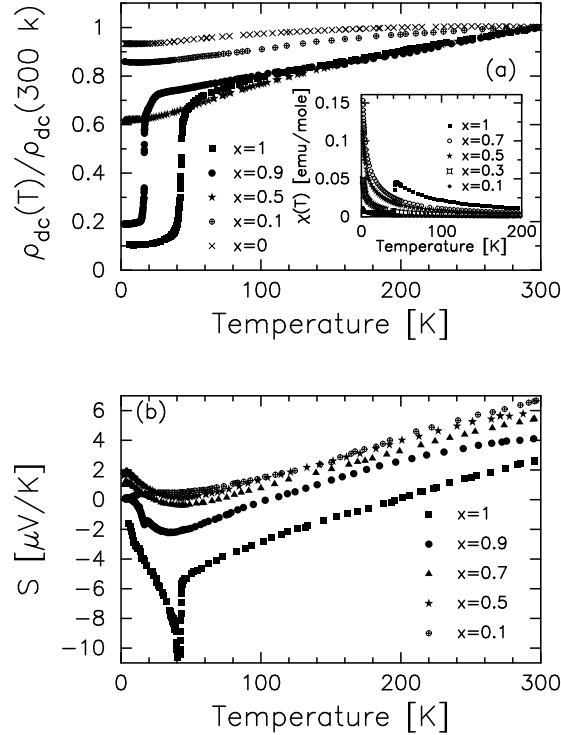


Figure 1. Panel (a) shows the resistivity and the magnetic susceptibility of $\text{Yb}_x\text{Y}_{1-x}\text{InCu}_4$ as function of temperature for various concentrations of Y ions (6). Note, all the “high-temperature” data can be collapsed onto a single universal curve, by normalizing the susceptibility with respect to an effective Yb-concentration (not shown). Panel (b) shows the thermopower of $\text{Yb}_x\text{Y}_{1-x}\text{InCu}_4$ as a function of temperature for various concentrations of Y ions (6).

The low-temperature phase ($T \leq T_v$) shows anomalies typical of an intermetallic compound with a fluctuating valence. The electronic specific heat and the susceptibility are enhanced (4); the ESR data (11) also indicates a large density of states at the Fermi level E_F . The electrical resistance and the Hall constant are small and metallic, and the low-temperature slope of the thermoelectric power is large (6). The optical conductivity is Drude like, with an additional structure in the mid-infrared range which appears quite suddenly at T_v (3), indicating a mixing of the f-states with the conduction band. Neither the susceptibility, nor the resistivity (6), nor the Hall constant (2) show any temperature dependence below T_v , i.e., the system

behaves as a fermi liquid with a characteristic energy scale $T_{FL} \gg T_v$. The magnetic moment of the rare earth ions is quenched in the ground state by the f-d hybridization but the onset of the high-entropy phase cannot be explained by the usual Anderson model in which the low- and high-temperature scales are the same and the spin degeneracy is not expected to be recovered below T_{FL} . In these valence-change systems, however, the f -moment at is recovered at $T_v \ll T_{FL}$.

The high- T phase that sets in at T_v is also anomalous. In doped systems, the susceptibility data above T_v can be represented by a single universal curve, provided one scales the data by an effective concentration of magnetic f -ions, which is smaller than the nominal concentration of f -ions. The functional form of the magnetic response agrees well with the “single-ion” crystal field (CF) theory for all values of the field. The Yb ions seem to be in the stable 3+ configuration with one f -hole and with the magnetic moment close to the free ion value $g_L \sqrt{J(J+1)} \mu_B = 4.53 \mu_B$ ($g_L = 8/7$ is the Landé factor and $J = 7/2$ is the angular momentum of the $4f^{13}$ hole). The dynamical susceptibility obtained from neutron scattering data (12) is typical of isolated local moments, with well resolved CF excitations(13).

The resistivity of $\text{Yb}_{1-x}\text{Y}_x\text{InCu}_4$ alloys exhibits a weak maximum and the thermopower has a minimum above 100 K but neither quantity shows much structure at low temperatures, where the susceptibility drops below the single-ion CF values. The discontinuity of the thermoelectric power at the valence transition is a trivial consequence of the different thermoelectric properties of the two phases: the thermopower of the valence-fluctuating phase has an enhanced slope and grows rapidly up to T_v , where it suddenly drops to values characteristic of the high-temperature phase. The resistivity is not changed much by a magnetic field up to 30 T (14). In typical Kondo systems, on the other hand, one expects a logarithmic behavior on the scale T/T_K and a large negative magnetoresistance. Here, despite the presence of the well defined local moments, there are no Kondo-like anomalies. The Hall constant of the $x = 0$ compound is large and negative in the high-temperature phase, typical of a semi-metal (2); the optical conductivity (3) shows a pronounced maximum of the optical spectral weight at a charge-transfer peak near 1 eV and a strongly suppressed Drude peak. The high-temperature ESR data for Gd^{3+} embedded in YbInCu_4 resemble those found in integer-valence semi-metallic or insulating hosts (15).

The hydrostatic pressure and the magnetic field give rise, like the temperature and the doping, to strong and often surprising effects. The critical temperature decreases with pressure (14) but the data cannot be explained with the Kondo volume collapse model (4). We mention also that doping the Yb sites with Lu^{3+} ions (5) reduces T_v despite the fact that Lu has a smaller ionic radius than Yb or Y; doping the In sites by smaller Ag ions

enhances T_v in $\text{YbIn}_{1-x}\text{Ag}_x\text{Cu}_4$ (8, 16) without changing appreciably the lattice parameter. Thus, the effects of doping can not be explained in terms of a chemical pressure. An external magnetic field of a critical strength $H_c(T)$ destabilizes the low-temperature phase and induces a metamagnetic transition which can be seen in the magnetoresistance and the magnetization data (4). The experimental values of $H_c(T = 0)$ and $T_v(H = 0)$ are of the same order of magnitude.

2. Theoretical description and the DMFT solution

A qualitative description of the properties described above is provided by the Falicov-Kimball (FK) model (17) which takes into account the interaction between a 2-fold degenerate conduction band and a lattice of Yb and Y ions. Each lattice site can be occupied either by a Yb^{2+} , Yb^{3+} or Y^{3+} ion. The Yb^{2+} ion has a full f-shell and is non-magnetic, the Yb^{3+} is magnetic with one f-hole in a $J=7/2$ spin-orbit state, and the Y^{3+} is non-magnetic, with one additional hole with respect to the Yb^{2+} ion. The number of Y^{3+} ions is fixed in each alloy, while the concentration of Yb^{3+} and Yb^{2+} ions is a thermodynamic variable. The f-holes are localized and the state of a given Yb ion can not change in time but the relative number of Yb^{2+} and Yb^{3+} changes due to thermodynamic fluctuations. The conduction electrons can hop between nearest-neighbor sites on the D-dimensional lattice, with a hopping matrix $-t_{ij} = -t^*/2\sqrt{D}$; we choose a scaling of the hopping matrix that yields a nontrivial limit in infinite-dimensions (18). We assume that the magnetic f-hole on Yb^{3+} and the spinless hole on Y^{3+} interact with the holes in the conduction band by a Coulomb repulsion U_f and U_Y , respectively. Averaging over all possible random distributions of Yb^{2+} , Yb^{3+} and Y^{3+} ions restores the translational invariance and leads to the Falicov-Kimball model for the lattice Yb-Y ions,

$$\mathcal{H}_{\text{FK}} = \mathcal{H}_d^0 + \mathcal{H}_f + \mathcal{H}_Y + \mathcal{H}_U, \quad (1)$$

where

$$\mathcal{H}_d^0 = \sum_{ij,\sigma} (-t_{ij} - \mu\delta_{ij}) d_{i\sigma}^\dagger d_{j\sigma}, \quad (2)$$

$$\mathcal{H}_f = \sum_{i,\eta} (E_f - \mu) f_{i\eta}^\dagger f_{i\eta}, \quad (3)$$

$$\mathcal{H}_Y = \sum_i (E_Y - \mu_Y) c_i^\dagger c_i, \quad (4)$$

and

$$\mathcal{H}_U = U_f \sum_{i,\sigma\eta} d_{i\sigma}^\dagger d_{i\sigma} f_{i\eta}^\dagger f_{i\eta} + U_Y \sum_{i,\sigma} d_{i\sigma}^\dagger d_{i\sigma} c_i^\dagger c_i. \quad (5)$$

Spin-1/2 conduction holes are created or destroyed at site i by $d_{i\sigma}^\dagger$ or $d_{i\sigma}$, the 8-fold degenerate localized f-holes are created or destroyed at site i by $f_{i\eta}^\dagger$ or $f_{i\eta}$, and the spinless Y-hole is created or destroyed at site i by c_i^\dagger or c_i . We use σ and η labels to denote the angular momentum state of the d- and f-holes, respectively. The d-, f- and Y-number operators at each site are $n_d^i = \sum_\sigma n_{d\sigma}^i$, $n_f^i = \sum_\eta n_{f\eta}^i$, and n_Y^i , respectively, and we have the local constraint $n_f^i + n_Y^i \leq 1$. The Y-doping reduces the number of f-holes in the conduction band and provides additional Coulomb scattering for conduction-holes. For a given concentration x of Y ions, the chemical potential μ is employed to conserve the total number of remaining d- and f-particles, $n_d(T) + n_f(T) = n_{tot} - x$. In the presence of a magnetic field the magnetic degeneracy of the f-holes is lifted and the Hamiltonian (1) is supplemented by a Zeeman term. Using the basis that diagonalizes simultaneously the zero-field Hamiltonian and $J_z^{7/2}$ component of the angular momentum operator, we can write,

$$\mathcal{H}_Z = g_d \mu_B H \sum_{i\sigma} \sigma d_{i\sigma}^\dagger d_{j\sigma} + g_f \mu_B H \sum_{i\eta} \eta f_{i\eta}^\dagger f_{i\eta}, \quad (6)$$

where g_d and g_f are the g-factors. The numerical calculations are performed for a hyper-cubic lattice with a Gaussian noninteracting density of states $\rho(\epsilon) = \exp[-\epsilon^2/t^{*2}]/(\sqrt{\pi}t^*)$; and t^* is taken as the unit of energy ($t^* = 1$). We consider only the homogeneous phase, where all quantities are translationally invariant.

The DMFT reduces an infinitely-dimensional FK lattice to the problem of an atomic d-state coupled to an atomic f-state by the same Coulomb interaction as on the lattice (19), and perturbed by an external time-dependent field, $\lambda(\tau, \tau')$. The field is taken in such a way that the local d-electron Green's function of the lattice coincides with the Green's function of the atomic d-state, $G_{loc}^\sigma(z) = G_{at}^\sigma(z)$. The atomic problem is solved by defining the generating functional (the partition function of the FK atom) in the interaction representation (20),

$$\mathcal{Z}_{at}(\mu, \lambda) = \text{Tr}_{dfc} \left[T_\tau e^{-\beta \mathcal{H}_{at}} S(\lambda) \right], \quad (7)$$

where the statistical sum runs over all possible quantum states of the system and depends on $\lambda^\sigma(\tau, \tau')$ for $\tau, \tau' \in (0, \beta)$. The Hamiltonian of the FK atom,

$$\begin{aligned} \mathcal{H}_{at} = & -\mu \sum_\sigma d_\sigma^\dagger d_\sigma + (E_f - \mu) \sum_\eta f_\eta^\dagger f_\eta + (E_Y - \mu_Y) c^\dagger c \\ & + U_f \sum_{\sigma\eta} d_\sigma^\dagger d_\sigma f_\eta^\dagger f_\eta + U_Y \sum_{\sigma\eta} d_\sigma^\dagger d_\sigma c^\dagger c, \end{aligned} \quad (8)$$

defines the time evolution of the operators, and the external field defines the time-evolution operator for the state vectors,

$$S(\lambda) = T_\tau e^{-\int_0^\beta d\tau \int_0^\beta d\tau' \sum_\sigma \lambda^\sigma(\tau, \tau') d_\sigma^\dagger(\tau) d_\sigma(\tau')}. \quad (9)$$

In the presence of the magnetic field, we add to (8) a Zeeman term that is obtained from (6) in an obvious way. The Hilbert space can be decomposed into invariant subspaces with respect to n_f and n_c , and the matrix elements in (7) can be calculated within the n_f -invariant subspace by replacing $\sum_\eta f_\eta^\dagger f_\eta$ in \mathcal{H}_{at} by its eigenvalue (0 or 1) and setting $n_c = 0$. Within the n_c -invariant subspace we use $n_f = 0$ and $n_c = 1$. This gives,

$$\mathcal{Z}_{\text{at}}(\mu, \lambda) = \mathcal{Z}_0(\mu, \lambda) + \mathcal{Z}_f \mathcal{Z}_0(\mu - U_f, \lambda) + \mathcal{Z}_Y \mathcal{Z}_0(\mu - U_Y, \lambda), \quad (10)$$

where, $\mathcal{Z}_f = \sum_\eta e^{-\beta(E_\eta^{(7/2)} - \mu)}$ and $\mathcal{Z}_Y = e^{-\beta(E_Y - \mu_Y)}$ are the partition functions of the Yb^{3+} and Y^{3+} holes decoupled from the d-states, and $\mathcal{Z}_0(\mu, \lambda)$ is the partition function of the $U_f = U_Y = 0$ atomic d-state coupled to the λ -field only. We have,

$$\mathcal{Z}_0(\mu, \lambda) = \prod_\sigma \mathcal{Z}_0^\sigma(\mu, \lambda), \quad (11)$$

where

$$\mathcal{Z}_0^\sigma(\mu, \lambda) = \text{Tr}_d \left[T_\tau e^{-\beta \mathcal{H}_0^\sigma} S(\mu, \lambda^\sigma) \right]. \quad (12)$$

and

$$\mathcal{H}_0^\sigma = - \sum_\sigma (\mu - g_d \mu_B H) d_\sigma^\dagger d_\sigma. \quad (13)$$

To calculate $\mathcal{Z}_0^\sigma(\mu, \lambda)$ we introduce the d-electron propagator for this simplified atomic problem,

$$G_0^\sigma(\tau, \tau') = - \frac{\delta \ln \mathcal{Z}_0^\sigma}{\delta \lambda^\sigma(\tau', \tau)}, \quad (14)$$

which is determined by the equations of motion (EOM) and the boundary condition $G_0^\sigma(\tau, \tau') = G_0^\sigma(\tau + \beta, \tau')$. The EOM's reduce, in the Matsubara representation, to a set of decoupled linear algebraical equations, such that $[G_{0n}^\sigma]^{-1} = [g_{0n}^\sigma]^{-1} - \lambda_n^\sigma$, where $[g_{0n}^\sigma]^{-1} = i\omega_n + \mu - \sigma \mu_B g_d H$ is the propagator of the trivial $U_f = U_Y = \lambda = 0$ atomic d-state. Using $\mathcal{Z}_0^\sigma(\mu, \lambda) = \det |[G_0^\sigma]^{-1}|$ and $\det |[g_0^\sigma]^{-1}| = 1 + \exp(\mu - \sigma \mu_B g_d H)$, we can write the partition function of the $U_f = U_Y = 0$, $\lambda \neq 0$ atomic model as,

$$\mathcal{Z}_0^\sigma(\mu, \lambda) = (1 + e^{\beta(\mu - \sigma \mu_B g_d H)}) \prod_n (1 - \lambda_n^\sigma g_{0n}^\sigma). \quad (15)$$

The partition functions in the $n_f = 1$ ($n_Y = 0$) and the $n_Y = 1$ ($n_f = 0$) subspaces are obtained from the $n_f = n_Y = 0$ solution by replacing μ in $\mathcal{Z}_0^\sigma(\mu, \lambda)$ by $\mu - U_f$ and $\mu - U_Y$, respectively.

The fully renormalized Green's function of the FK atom is, by definition,

$$G^\sigma(\tau, \tau') = -\frac{1}{\mathcal{Z}_{at}(\mu, \lambda)} \frac{\delta \mathcal{Z}_{at}(\mu, \lambda)}{\delta \lambda^\sigma(\tau', \tau)}, \quad (16)$$

and can be calculated using Eqs.(10) and (14). In Matsubara representation, where $G_{0n}^\sigma = -\delta \ln \mathcal{Z}_0^\sigma / \delta \lambda_n^\sigma$, we obtain

$$G_{at}^\sigma(i\omega_n) = N_0 G_0^\sigma(i\omega_n) + \frac{N_f}{[G_0^\sigma(i\omega_n)]^{-1} - U_f} + \frac{N_Y}{[G_0^\sigma(i\omega_n)]^{-1} - U_Y}, \quad (17)$$

where $N_0 = \mathcal{Z}_0(\mu, \lambda) / \mathcal{Z}_{at}$, $N_f = \mathcal{Z}_f \mathcal{Z}_0(\mu - U_f, \lambda) / \mathcal{Z}_{at}$, and $N_Y = \mathcal{Z}_Y \mathcal{Z}_0(\mu - U_Y, \lambda) / \mathcal{Z}_{at}$ are the respective average numbers of the Yb^{2+} , Yb^{3+} and Y^{3+} ions in a Y-doped system. The concentration of Y-ions, $N_Y = x$, is kept constant at each temperature. For a given concentration Y ions we calculate $G_{at}^\sigma(i\omega_n)$ using $N_0 = 1 - N_f - x$. Since G_0^σ is the solution of the $U_f = U_Y = 0$, $\lambda \neq 0$ problem, the self energy of the full atomic problem is given by the Dyson equation,

$$\Sigma^\sigma = [G_0^\sigma]^{-1} - [G_{at}^\sigma]^{-1}. \quad (18)$$

The solution for the FK lattice is defined by λ such that

$$G_{at}^\sigma(i\omega_n) = \int \frac{\rho(\epsilon)}{i\omega_n + \mu + \sigma \mu_B g_d H - \Sigma^\sigma(z) - \epsilon} d\epsilon. \quad (19)$$

The equations (17) and (18), together with the expressions (10) and (15) for the partition function, and the self-consistency condition (19), can be solved by iteration. One starts from some trial self energy and finds G_{at}^σ using Eq.(19). Then, one finds G_0^σ from Eq.(18), finds $\mathcal{Z}_{at}(\mu, \lambda)$ from (10) and (15), calculates G_{at}^σ by functional derivatives, recalculates Σ^σ using (18), and continues until the fixed point is reached. Once the numbers N_0 and N_f are obtained we can iterate (17), (18) and (19) on the real axis and find the retarded quantities. In what follows, we use the DMFT to calculate the thermodynamic and transport properties of the model corresponding to the $\text{Yb}_{1-x}\text{Y}_x\text{InCu}_4$ alloys.

3. Numerical results

The calculations are performed assuming that doping by Y^{3+} ions removes holes from the conduction band. In an undoped sample the total number of conduction holes and the holes on the Yb^{3+} ions is $n_d + n_f = 1.5$, while for a concentration x of Y ions we assume $n_d + n_f = 1.5 - x$. The

parameter space of the model is very large and a quantitative comparison would require a fine-tuning of the parameters. Here, we only show the results for static correlation functions obtained for $U_f = U_Y = 2t^*$, and $E_f = -0.6t^*$. Panel (a) of Fig.2 shows the effect of temperature and doping

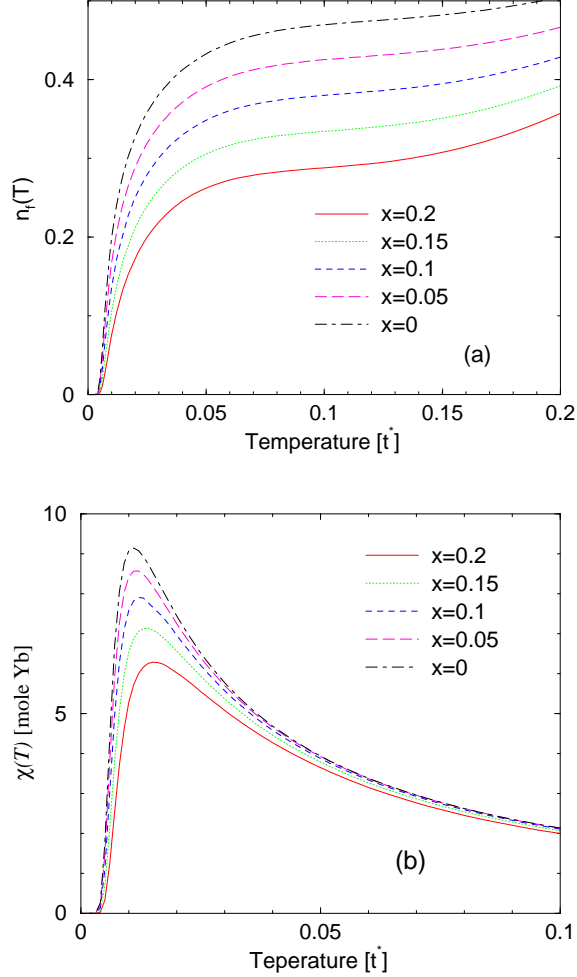


Figure 2. Panel (a) shows localized electron filling for eightfold degenerate doped Falicov-Kimball model with $U_f = U_Y = 2t^*$, $E_f = -0.6t^*$, and various doping levels x . Panel (b) shows spin susceptibility normalized to the nominal concentration of Yb ions in a $\text{Yb}_{1-x}\text{Y}_x\text{InCu}_4$ alloy.

on the average concentration of Yb^{3+} ions. Panel (b) shows the f-electron contribution to the spin susceptibility, which vanishes below T_v , and is Curie-like for $T \gg T_v$. Above the transition temperature, defined by the

inflection point of the susceptibility curves, the concentration of Yb^{3+} ions becomes significant but the effective Curie constant decreases with doping. The effect of doping and temperature on transport properties is shown in

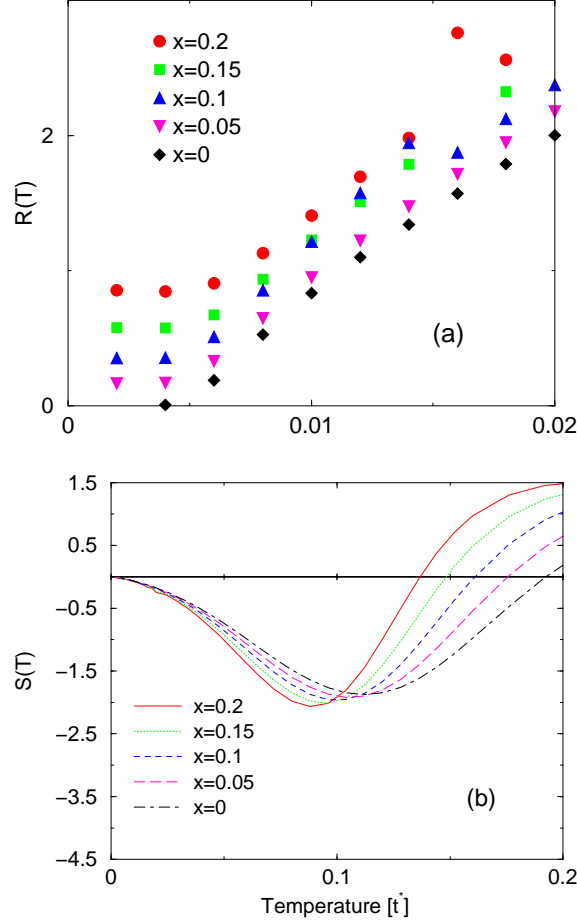


Figure 3. Panel (a) shows DC resistivity of the Falicov-Kimball model for the same parameters as in Fig.(2.) Panel (b) shows thermopower.

Fig. 3. Panel (a) shows that the resistivity of an undoped ($x = 0$) sample starts from zero and becomes large around T_v , where the concentration of Yb^{3+} ions is large. In doped ($x > 0$) samples, the residual resistivity is finite. At high temperatures the resistivity of all samples has a maximum (not shown here). The relative importance of the doping diminishes for $T \geq T_v$. The thermopower results are shown in panel (b), using a 10 times larger temperature scale than in panel (a), to reveal the minimum and a sign-change. The theoretical results shown in Figs. 2 and 3 have a number

of qualitative features that one finds in the experimental data. A detailed comparison will be published elsewhere.

Acknowledgements

We acknowledge useful discussions with C. Geibel and J. Sarrao. We acknowledge the support by the National Science Foundation under grant DMR-0210717. V.Z. acknowledges the support by the Swiss National Science Foundation, grant no. 7KRPJ65554.

References

1. I. Felner and I. Novik, Phys. Rev. B **33**, 617 (1986)
2. E. Figueroa, J. M. Lawrence, J. Sarrao and Z. Fisk, M. F. Hundley and J. D. Thompson, Solid State Commun. **106**, 347 (1998)
3. S. R. Garner, J. N. Hancock, Y.W. Rodriguez, Z. Schlesinger, B. Bucher, Z. Fisk and J. L. Sarrao, Phys. Rev. B **63**, R4778 (2000)
4. J. L. Sarrao, Physica B **259** & **261**, 129 (1999)
5. W. Zhang, N. Sato, K. Yoshimura, A. Mitsuda, T. Goto and K. Kosuge, Phys. Rev. B **66**, 024112-1 (2002)
6. M. Očko and J. L. Sarrao, Physica B **312** & **313**, 341 (2002)
7. C. Dallera, M. Grioni, A. Shukla, G. Vankó, J. L. Sarrao, J. P. Rueff and D. L. Cox, Phys. Rev. Lett. **88**, 196403 (2002)
8. A. L. Cornelius, J. M. Lawrence, J. Sarrao, Z. Fisk, M. F. Hundley, G. H. Kwei, J. D. Thompson, C. H. Booth and F. Bridges, Phys. Rev. B **56**, 7993 (1997)
9. J. M. Lawrence, S. M. Shapiro, J. L. Sarrao and Z. Fisk, Phys. Rev. **55**, 14467 (1997)
10. A. Mitsuda, T. Goto, K. Yoshimura, W. Zhang, N. Sato, K. Kosuge and H. Wada, Phys. Rev. Lett. **88**, 137204 (2002)
11. C. Rettori, S. B. Oseroff, D. Rao, P. G. Pagliuso, G. E. Barberis, J. Sarrao, Z. Fisk and M. F. Hundley, Phys. Rev. B **55**, 1016 (1997)
12. E. A. Goremychkin and R. Osborn, Phys. Rev. B **47**, 14280 (1993)
13. A. Murani, D. Richard and R. Bewley, Physica B **312** & **313**, 346 (2002)
14. C. D. Immer, J. Sarrao, Z. Fisk, A. Lacerda, C. Mielke and J. D. Thompson, Phys. Rev. B **56**, 71 (1997)
15. T.S. Altshuler, M.S. Bresler, M. Schlott, B. Elschner and E. Grady, Z. Phys. B **99**, 57 (1995)
16. J. M. Lawrence, R. Osborn, J. L. Sarrao and Z. Fisk, Phys. Rev. **59**, 1134 (1999)
17. L. M. Falicov and J. C. Kimball, Phys. Rev. Lett. **22**, 997 (1969).
18. W. Metzner and D. Vollhardt, Phys. Rev. Lett. **62**, 324 (1989)
19. U. Brandt and C. Mielsch, Z. Phys. B **75**, 365 (1989);
20. L.P. Kadanoff and G. Baym, *Quantum Statistical Physics* (W. A. Benjamin, Menlo Park, CA, 1962).
21. J. Freericks and V. Zlatić, Phys. Rev. B **58**, 322 (1998); V. Zlatić and J. Freericks, in *Proc. NATO ARW Conference, Bled 2000*, edited by P. Prelovsek, S. Sarkar, J. Bonca (North-Holland, Amsterdam, 2001).